

AERODYNAMIC STABILITY OF A SUPER LONG-SPAN BRIDGE WITH SLOTTED BOX GIRDER

by

Hiroshi SATO¹⁾, Nobuyuki HIRAHARA²⁾, Koichiro FUMOTO³⁾, Shigeru HIRANO⁴⁾ and Shigeki KUSUHARA⁵⁾

ABSTRACT

Aerodynamic stability is one of the most important themes in the design of super long-span bridges. In order to improve the aerodynamic stability, various researches were conducted and it was confirmed that slotted box girder with some devices shows the good aerodynamic stability. In this paper, the results of full aeroelastic model test and flutter analysis for a generic super long-span bridge, whose main span is 2.8km, are described. And it was confirmed that slotted box girder was applicable for the super long-span bridge from the reason that it is excellent in economical efficiency and aerodynamic stability.

KEYWORD: aerodynamic stability; super long-span bridge; flutter analysis; full aeroelastic model; slotted box girder

1. INTRODUCTION

There are several plans or ideas of strait crossing road projects in Japan. In these projects, super long-span bridges longer than the Akashi Kaikyo Bridge may be included. In the design of such super long-span bridges, aerodynamic stability is one of the most important themes. Furthermore, reduction of construction cost is also required. Therefore, Independent Administrative Institution Public Works Research Institute (IAIPWRI) and Honshu-Shikoku Bridge Authority (HSBA) have been conducting cooperative study on super structure of super long-span bridges that have good aerodynamic stability and economical efficiency.

In the previous studies [1][2] by the authors, it was found that a slotted box girder with some

devices has good aerodynamic characteristics. Therefore, the slotted box girder was applied to a generic super long-span bridge, and full aeroelastic model test was conducted. And the result was compared with 3-dimensional flutter analysis.

In this paper, main results of the previous study on the slotted box girders are outlined first. Then the results of full aeroelastic model test and flutter analysis for a generic super long-span bridge, whose main span is 2.8km, are described.

2. FLUTTER CHARACTERISTICS OF SLOTTED BOX GIRDERS [1]

The effect of location and size of slot on aerodynamic characteristics was examined through section model wind tunnel tests. Reduced mass $\mu (=m/(B^2))$, m : mass per unit length, ρ : air density, B : girder width), reduced polar moment of inertia $(=I/(B^4))$, I : polar

-
- 1) Director, Structures Research Group, Public Works Research Institute, Independent Administrative Institution
 - 2) Manager, Maintenance Planning Division, Maintenance Department, Honshu-Shikoku Bridge Authority (Formerly, Leader of Bridge Structure Research Team, Structures Research Group, ditto)
 - 3) Senior Research Engineer, Bridge Structure Research Team, ditto
 - 4) Director, Tarumi Maintenance Work Office, The 1st Maintenance Bureau, Honshu-Shikoku Bridge Authority (Formerly, Manager, Engineering Management Division, Long-span Bridge Engineering Center, HSBA)
 - 5) Deputy Manager, Engineering Management Division, ditto

moment of inertia per unit length), and natural frequency ratio ($\omega = f_z / f_t$, f_t : torsional natural frequency, f_z : vertical bending natural frequency) were 16, 2.1, and 2.1, respectively. The cross section of the model is shown in Fig.1. From the test results, it was found that the slot at the center increased the flutter onset wind speed. It was also found that the flutter onset wind speed was increased with the width of slot at the center of the girder (Fig.2).

In order to understand the effect of slot at the center of girder, preliminary analysis was conducted for slotted plate. For the analysis, aerodynamic forces acting on each plate was calculated using the Theodorsen's function. The aerodynamic interference between the 2 boxes was neglected. Using these aerodynamic forces, two degree-of-freedom flutter analysis was conducted by U-g method. The result of the flutter analysis (Fig.2) indicated that the flutter onset wind speed increased with size of slot. The differences between the analysis and the experiment seemed to be caused by aerodynamic interference between the 2 boxes.

Although wide slot at the center of the girder improves flutter characteristics, narrower slot would be preferable from the viewpoint of construction cost of towers and foundations. To improve aerodynamic characteristics, the effect of some devices was studied by section model tests. The tested devices are illustrated in Fig.3. The results showed that the center barrier and guide vanes improved flutter characteristics very well (Fig.4). However, the flutter speed was not so high when angle of attack was -3 deg. It was found that the guard rails at the bottom deck increased the flutter speed considerably at this angle of attack (Fig.5).

3. UNSTEADY AERODYNAMIC FORCES OF SLOTTED BOX GIRDERS [2]

From the above studies, it was found that slotted plates and slotted box girders have better flutter characteristics than single plates and single box girders. It was also found that the devices such as center barrier and guide vanes are effective to improve flutter characteristics of slotted box girders.

In order to understand causes of flutter characteristics of slotted plates and box girders

more precisely, unsteady aerodynamic forces were measured for three models: model A (single box girder, $b=0$ in Fig.1), model B (slotted box girder, $b=0.22B$ in Fig.1) and model C (slotted box girder with devices, Fig.3). The measurement was made by forced oscillation method with angle of attack 0 degree. Coefficients of the unsteady aerodynamic forces were defined as follows:

$$L = \{B^2[L_{ZR} \ddot{z} + L_{ZI} \dot{z}'] + B^3[L_R \ddot{\theta} + M_I \dot{\theta}']\} \quad (1.1)$$

$$M = \{B^3[M_{ZR} \ddot{z} + M_{ZI} \dot{z}'] + B^4[M_R \ddot{\theta} + M_I \dot{\theta}']\} \quad (1.2)$$

where, L : lift (upward positive), M : aerodynamic moment (head up positive), z : vertical displacement (upward positive), θ : torsional displacement (head up positive), ω : circular frequency, $(\)'$: $d(\)/dt$, L_{xx} or M_{xx} : coefficients of unsteady aerodynamic forces (z : caused by vertical vibration, θ : caused by torsional vibration, R : in phase with displacement, I : in phase with velocity).

In general, it is difficult to predict coupled flutter characteristics directly from these coefficients. For 2-degrees of freedom system, Nakamura [3] showed approximate relationship between unsteady aerodynamic coefficients M_{ZI} , M_I , L_R and M_R and some flutter properties as follows:

$$a = \frac{2M_{ZI}X}{L_R} - \frac{2M_I}{L_R} \quad (2.1)$$

$$X = \frac{z_0}{L_R} \frac{\omega_0/B}{(-1 + (\omega_z/\omega)^2)^2} \mu \quad (2.2)$$

$$\frac{2}{1 + M_R} (\omega_z/\omega)^2 \quad (2.3)$$

where, a : aerodynamic damping in logarithmic decrement.

If onset of flutter is defined as $a = 0$, simpler condition for onset of flutter can be derived from (2.1)-(2.3) as follows:

$$M_{ZI} L_R / M_I + M_R = 1 \quad (3.1)$$

$$\left(\frac{2}{(\mu^2 - 1)} \right) \left(\frac{1}{\mu} \right) \quad (3.2)$$

$$\left(\frac{1}{(\mu^2 - 1)} \right) \left(\frac{1}{\mu} \right) \quad (3.3)$$

The left hand side of inequality (3.1) was calculated for the Models A, B and C using measured unsteady aerodynamic forces, as well as for single plate and slotted plate using the Theodorsen's function. μ , μ and μ were assumed as 2.0, 15 and 2.0, respectively. The results are shown in Fig.6. The slotted box girders and slotted plate show higher flutter speed than the single box girder or single plate. Since the first term of the left hand side of inequality (3.1) is much larger than the second term, it can be said that this higher flutter speed was caused mainly by the property of $M_{ZI} L_R / M_{I1}$.

In Fig.8, reduced flutter speed $U/(fB)$ of slotted box girder with devices is almost identical with that of slotted box girder. In Fig.7, the results are plotted with $f B/U$. Flutter speed of slotted box girder with devices is higher than that without devices. It means that the effect of devices came from small value of M_{R} , which affected apparent frequency in wind as was shown in Equation (2.3).

4. WIND TUNNEL STUDY WITH A FULL AEROELASTIC MODEL

4.1 Full aeroelastic model

A suspension bridge, whose main span length is 2,800m and total length is 5,000m (Fig.8), was assumed as a prototype bridge of this study. The cross section of stiffening girder is shown in Fig.9. This box girder has 4-lanes, whose 2-lanes are on the grating installed on the slot in consideration of economical efficiency.

Wind tunnel test was conducted at the large boundary wind tunnel facility in Tsukuba. It was built in 1991 as one of the cooperative efforts between PWRI and HSBA in order to verify the aerodynamic stability of super long-span bridge such as the Akashi Kaikyo Bridge, and to establish the wind resistant design method for super long-span bridges considering 3-dimensional effects of structure and flow. The test section of this wind tunnel is 41m wide, 4m high and 30m long, and maximum wind speed is

12m/s. It is one of the largest boundary layer wind tunnels in the world.

The scale ratio of a full aeroelastic model of the assumed super long-span bridge was 1/125. Structural dimensions of the bridge and the model are shown in Table 1.

4.2 Wind tunnel test results for the full aeroelastic model

Static deformation by wind load is shown in Fig.10 and Photo 1. Large horizontal deformation (leeward side) and large torsional deformation (head down) were measured at the center of main span.

Logarithmic decrement at each wind speed is shown in Fig.11. It increased gradually with wind speed, and began decreasing at wind speed of about 6m/s. After that, logarithmic decrement decreased, and changed to negative value at 8.8m/s, and flutter started. According to the similarity law of Froude's number, flutter speed for the assumed bridge would be about 100m/s.

5. FLUTTER ANALYSIS FOR THE FULL AEROELASTIC MODEL

3-dimensional flutter analysis for the full aeroelastic model was conducted by using the measured unsteady aerodynamic forces. The analytical method was the same with the one that was used for the Akashi Kaikyo Bridge [4]. The conditions of 3-dimensional flutter analysis are shown in Table 2. In the analysis, static deformation was calculated first, then unsteady aerodynamic forces corresponding to attack angle of the girder were introduced. After that, eigenvalues were calculated using 50 vibrational modes in still air.

The analytical results of static deformation were shown in Fig.12. As for horizontal displacement and vertical displacement, the analytical values agreed well with experimental values. However, the analytical value (absolute value) for the torsional deformation was a little smaller than experimental value. Since aerodynamic characteristics are sensitive to attack angles, the flutter analysis was carried out using the measured torsional deformation.

The change of apparent damping of the 1st

torsional symmetrical mode (mode 19) is shown in Fig.13 by triangle mark. The flutter speed from the 3-dimensional flutter analysis was 7.9m/s. It agreed fairly well with the experiment.

Since the mass and polar moment of inertia of the model were larger than the values required from the similarity laws, flutter analysis was conducted for the required values of the model. The flutter speed was 7.6m/s. Therefore, flutter speed for the assumed bridge would be estimated about 85m/s, which confirmed its aeroelastic stability

6. CONCLUSIONS

Full aeroelastic model test and 3-dimensional flutter analysis was conducted for a generic super long-span bridge. Results and conclusions obtained are summarized as follows:

1) The slotted box girder was applied to a generic super long-span bridge, whose main span length was assumed to be 2.8km. Wind tunnel study was conducted with a 1/125 full aeroelastic model in smooth flow. It was confirmed that its flutter speed was high enough.

2) Three-dimensional flutter analysis was conducted for the full aeroelastic model. In the analysis, unsteady aerodynamic forces corresponding to attack angles of the girder deformed by steady wind forces were introduced. The calculated flutter speed agreed fairly well with the experiment.

In order to predict the torsional deformation and the flutter speed more accurately, improvement of the analytical model for the bridge is in progress.

REFERENCES

- [1] Sato H. and Ogihara K., Aerodynamic characteristics of slotted box girders, Proceedings of the 28th Joint Meeting of the Panel on Wind and Seismic Effects, UJNR, 1996
- [2] Sato H., Ogihara K. and Ogi K., Consideration on flutter characteristics of super long-span bridges, Proceedings of the 30th Joint Meeting of the Panel on Wind and Seismic Effects, UJNR, 1998

- [3] Nakamura, Y., An analysis of binary flutter of bridge deck sections, J. of Sound and Vibration, 57(4), 1978
- [4] Miyata T., Sato H. et al., Full model wind tunnel study on the Akashi Kaikyo Bridge, Proceedings of the 9th International Conference on Wind Engineering, 1995, pp.793-798

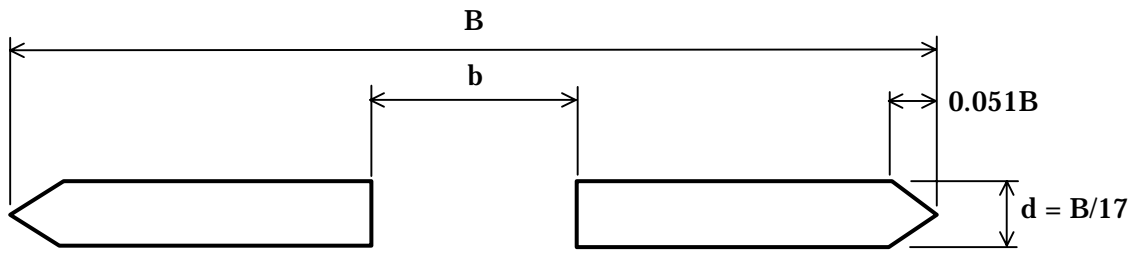


Fig.1 Cross Section of Slotted Girder

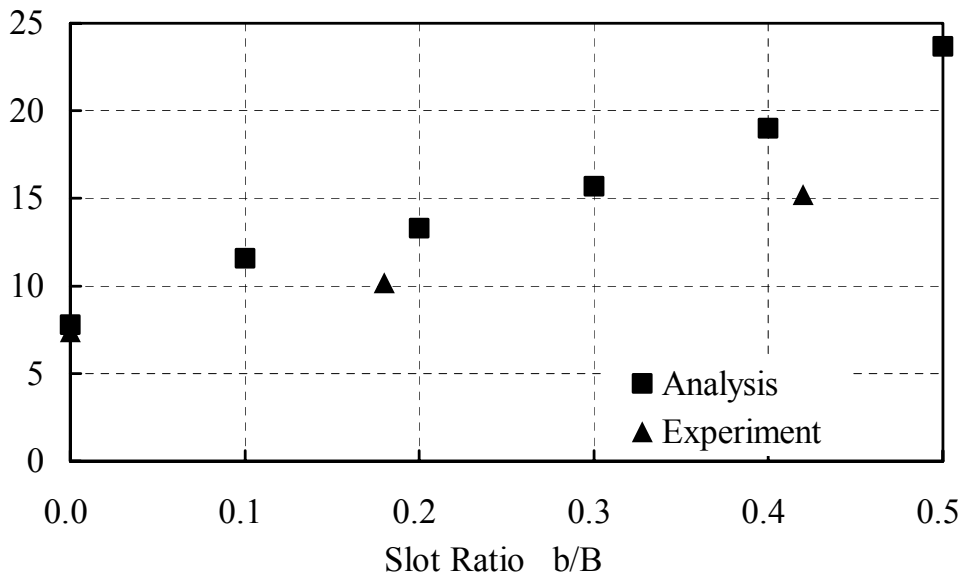


Fig. 2 Flutter Onset Speed and Slot Ratio

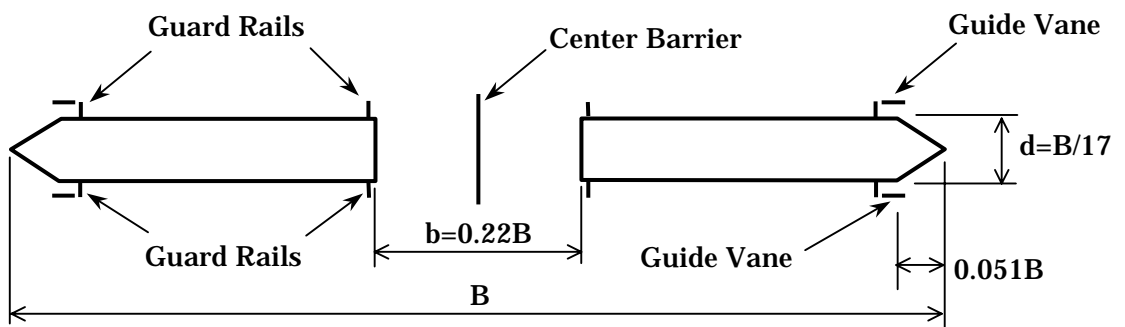


Fig.3 Slotted Box Girder with Devices

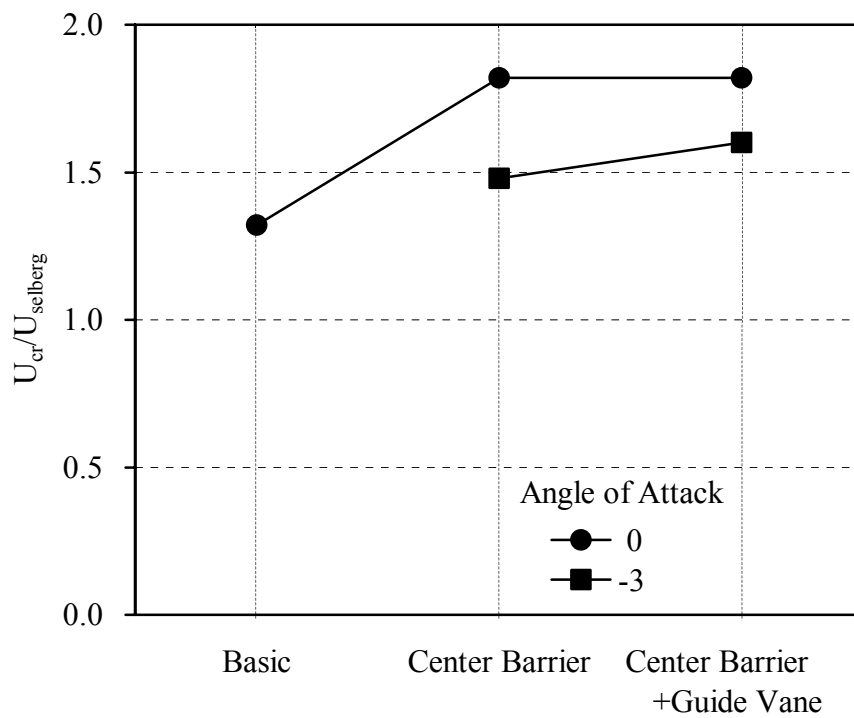


Fig.4 Effect of Tested Devices

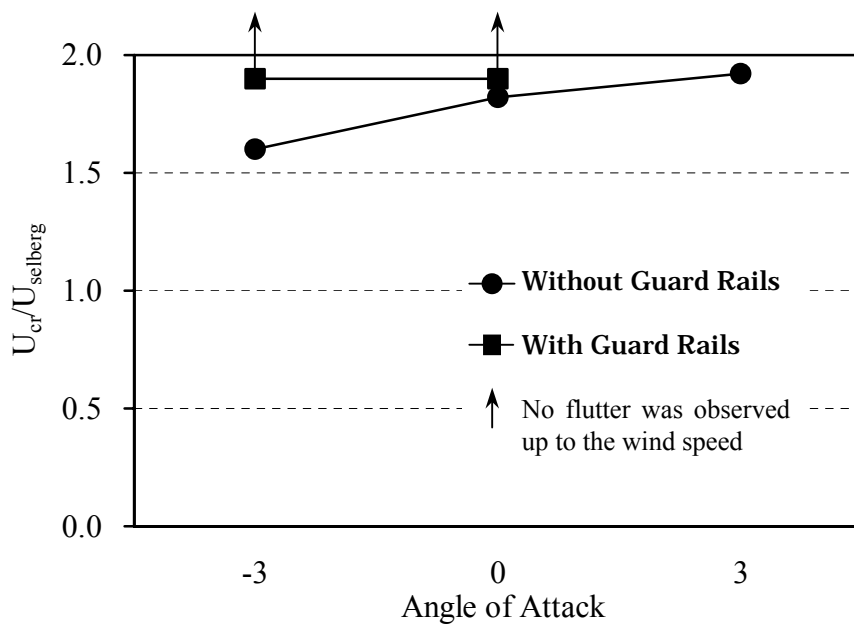
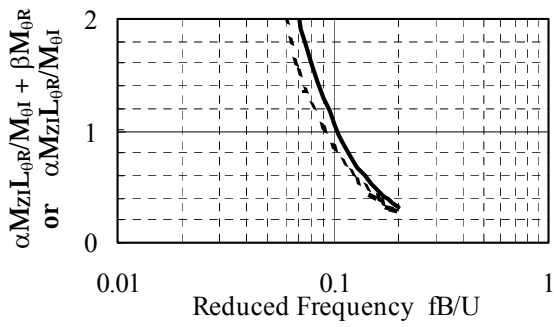
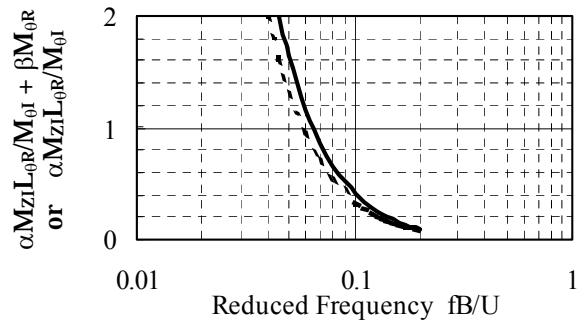


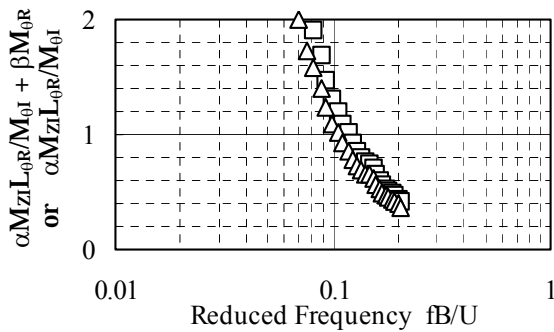
Fig.5 Effect of Guard Rails at Bottom Deck



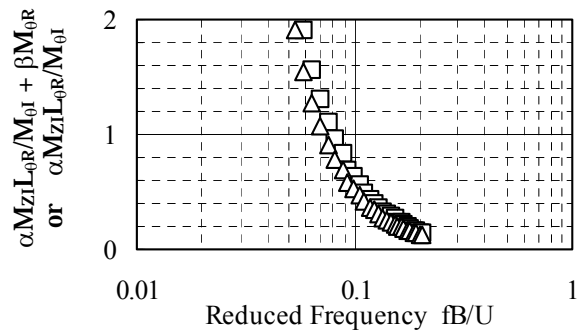
(a) Single Plate



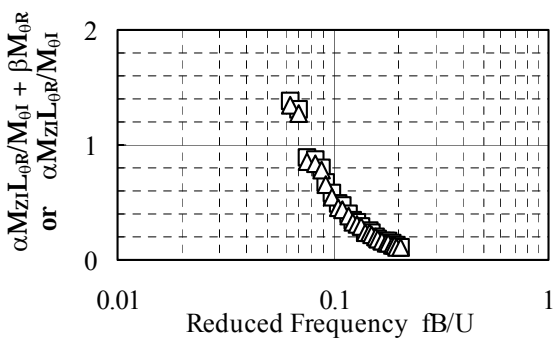
(b) Slotted plate



(c) Single Box Girder



(d) Slotted Box Girder



(e) Slotted Box Girder with Devices

— □ : $\alpha M_{ZI}L_{0R}/M_{0I} + \beta M_{0R}$
 - - - △ : $\alpha M_{ZI}L_{0R}/M_{0I}$

Fig.6 Prediction of Flutter Onset (plotted with fB/U)
 [Flutter with take phase when : $\alpha M_{ZI}L_{0R}/M_{0I} + \beta M_{0R} = 1$]

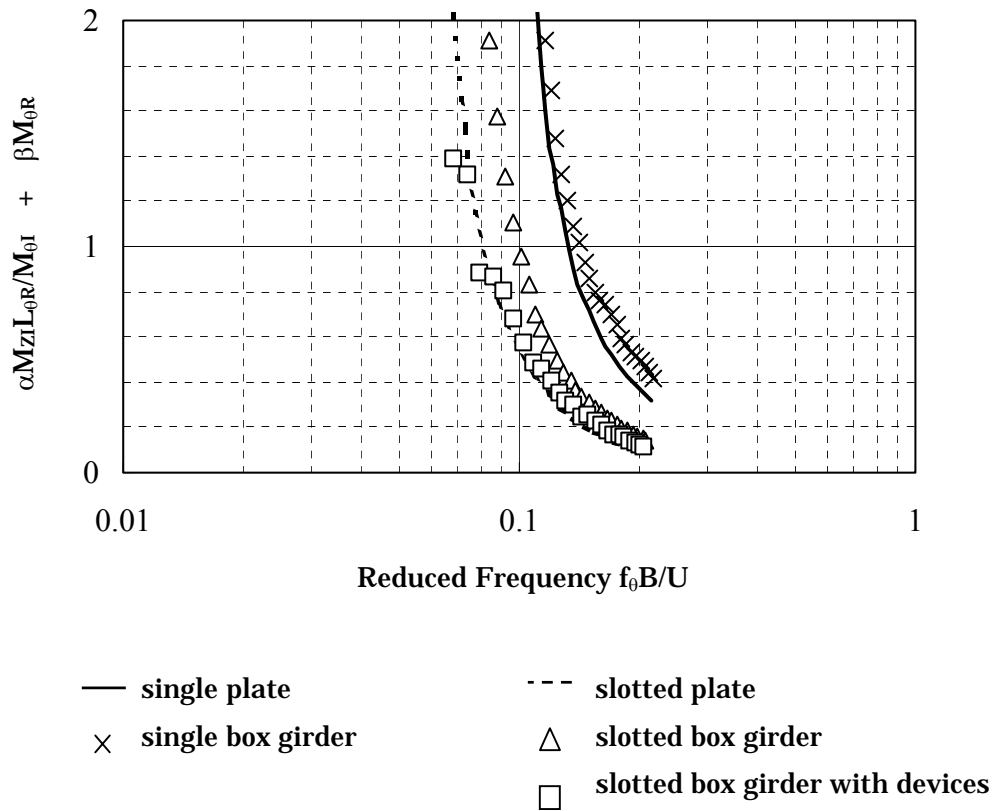


Fig.7 Prediction of Flutter Onset (plotted with $f_{\theta}B/U$)
 [Flutter with take place when $\alpha M_{ZIL_{0R}}/M_{\theta I} + \beta M_{\theta R} = 1$]

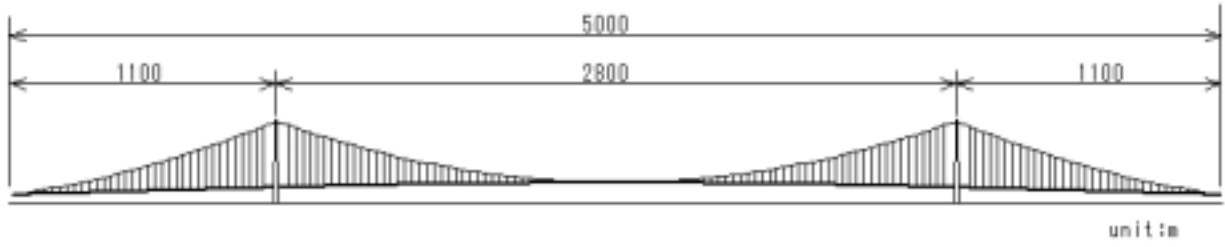


Fig. 8 Assumed super long-span bridge

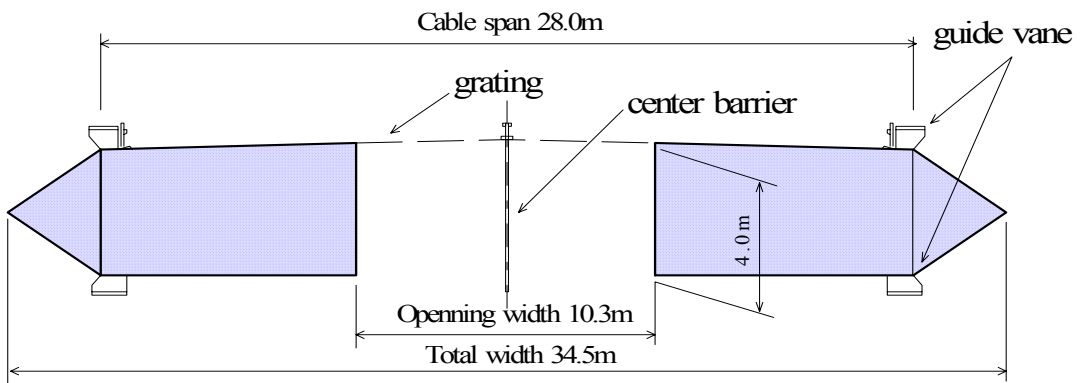


Fig. 9 Cross section of slotted box girder

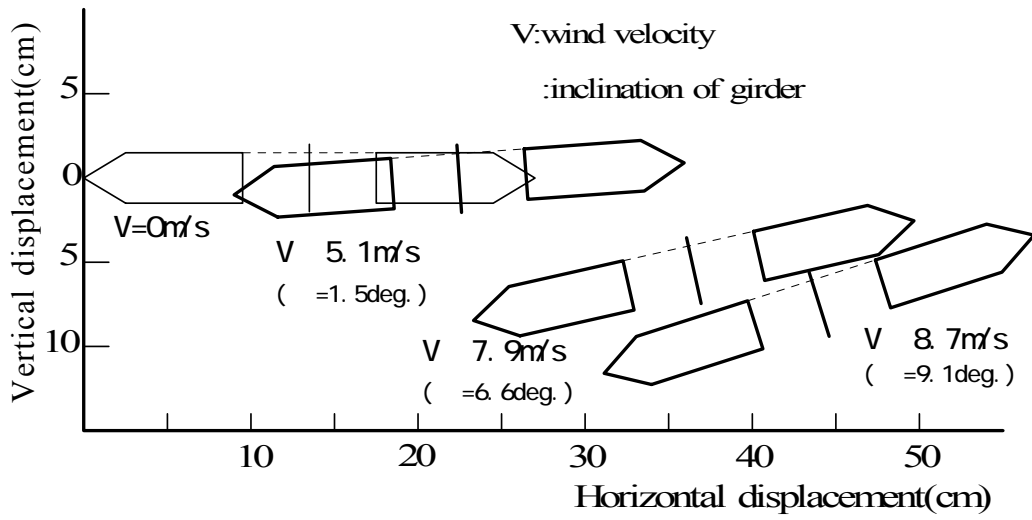


Fig.10 Deformation of girder

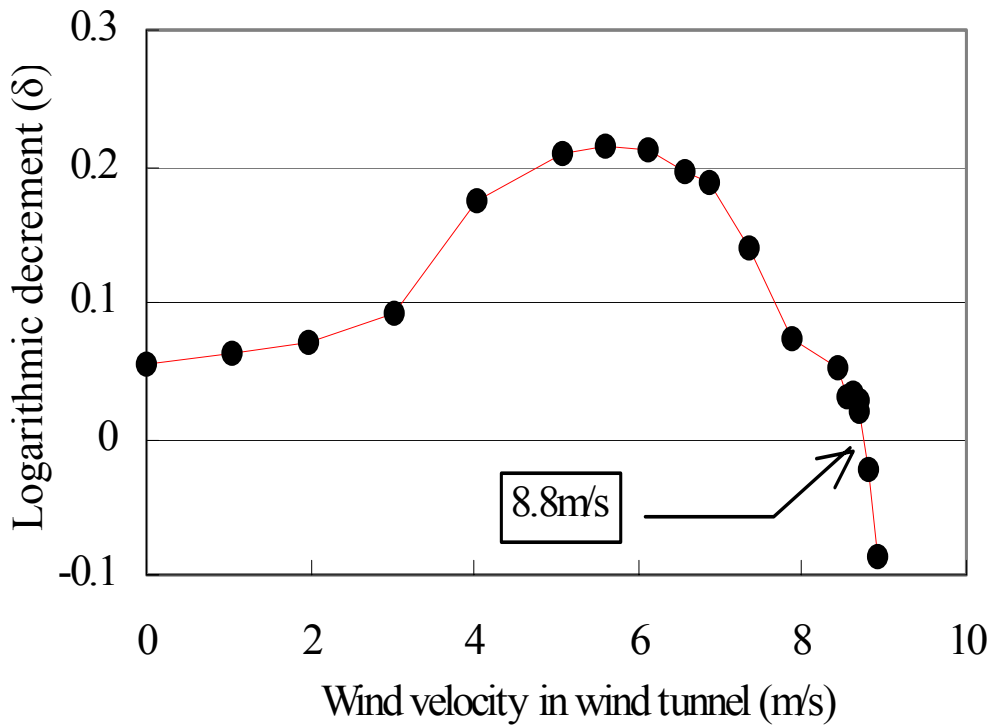


Fig. 11 Apparent damping – wind velocity

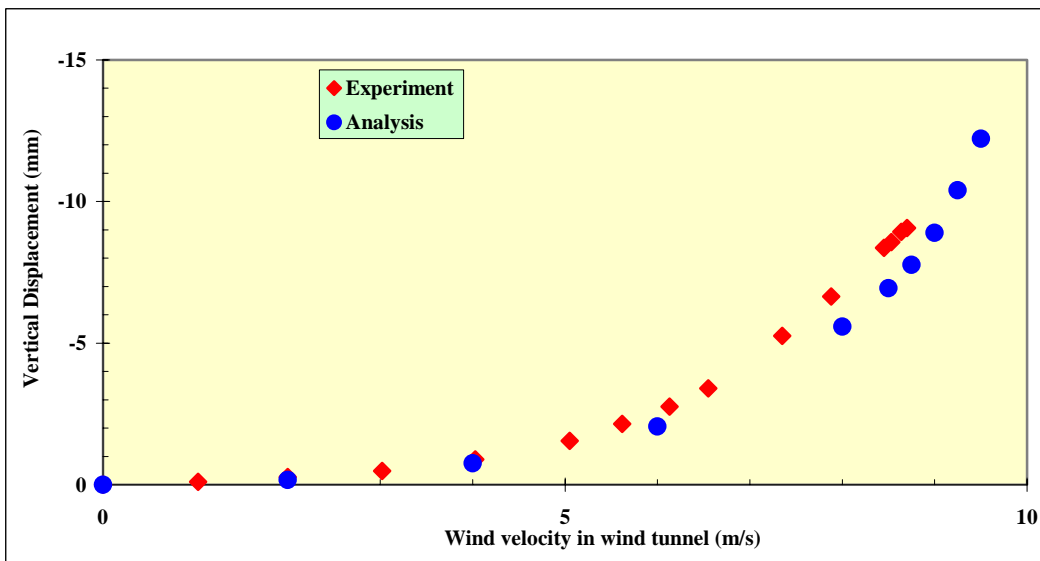
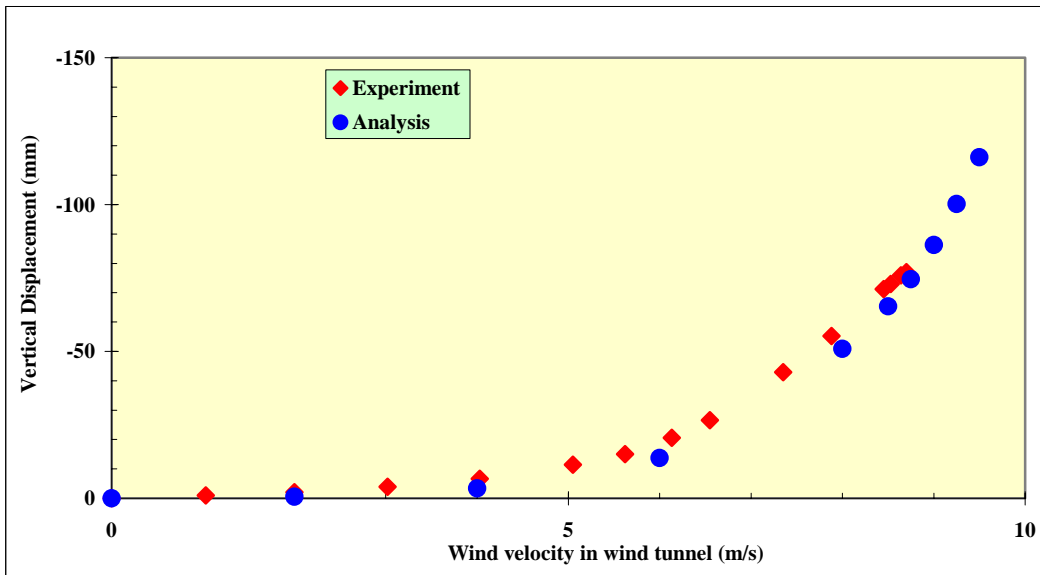
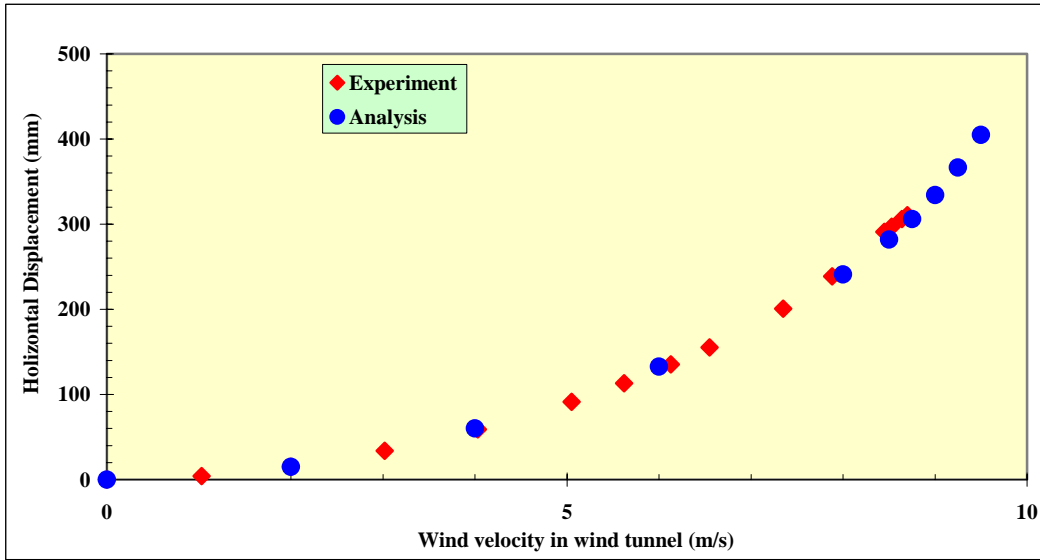


Fig. 12 Results of static deformation

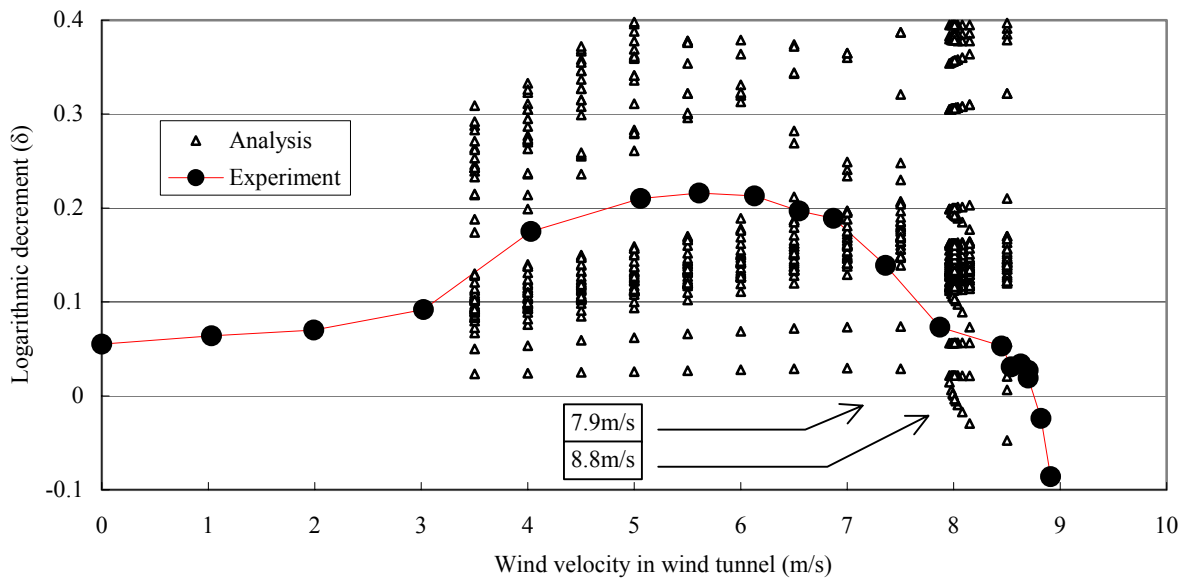


Fig. 13 Apparent damping – wind velocity (1st torsion symmetrical mode)



Photo 1 Static deformation of super long-span bridge (wind speed=8m/s)

Table 1 Structure dimensions of super long-span bridge

		Assumed bridge	Model value		(b)/(a)	
			Required (a)	Measured (b)		
Scale		-	1/125	1/125	-	
Mass		M	28.41t/m	1.818kg/m	2.100kg/m	1.156
Polar moment of inertia		I_p	$388t \cdot m^2/m$	$0.00159kg \cdot m^2/m$	$0.00246kg \cdot m^2/m$	1.547
Girder size	Width	B	34.5m	0.276m	0.276m	1.000
	Depth	D	4.0m	0.032m	0.032m	1.000
Stiffness	Vertical	EI_V	$1.707kNm^2/box$	$9.384Nm^2/box$	$12.277Nm^2/box$	1.308
	Horizontal	EI_H	$3.107kNm^2/box$	$48.828Nm^2/box$	$12.277Nm^2/box$	0.251
	Torsional	GJ	$1.090kNm^2/box$	$6.906Nm^2/box$	$6.853Nm^2/box$	0.992
Natural frequency	Vertical	1 st	0.0621Hz	0.693Hz	0.674Hz	0.973
		2 nd	0.0990Hz	1.111Hz	1.106Hz	0.995
		[1st]	0.0610Hz	0.683Hz	0.703Hz	1.029
		[2nd]	0.0831Hz	1.499Hz	1.494Hz	0.997
	Torsional	1 st	0.1256Hz	1.369Hz	1.321Hz	0.965
		[1st]	0.1466Hz	1.600Hz	1.597Hz	0.998
	Horizontal	1 st	0.0316Hz	0.352Hz	0.352Hz	1.000
		[1st]	0.0550Hz	0.502Hz	0.491Hz	0.978

[] means asymmetrical mode

Table 2 The conditions of flutter analysis

Item	Analysis condition																
Analytical method	Mode combination method. Using lower 50 modes.																
Air density	0.12 kg/m ³																
Structural damping	All modes $\zeta=0.02$																
Coefficients of aerodynamic forces	Main girder																
	<table border="1"> <tr> <td>Force</td> <td>Vertical</td> <td>Torsional</td> <td>Horizontal</td> </tr> <tr> <td>Lift</td> <td></td> <td></td> <td></td> </tr> <tr> <td>Moment</td> <td></td> <td></td> <td></td> </tr> <tr> <td>Drag</td> <td></td> <td></td> <td></td> </tr> </table>	Force	Vertical	Torsional	Horizontal	Lift				Moment				Drag			
	Force	Vertical	Torsional	Horizontal													
	Lift																
	Moment																
Drag																	
;Unsteady aerodynamic forces																	
;Quasi-steady aerodynamic forces																	
Cable Quasi-steady drag and lift force ($C_D=0.7$)																	
Tower Not considered																	